DESIGN AND DEVELOPMENT OF FRETTING FATIGUE TEST APPARATUS

Prithvi Raj Arora, M. S. D. Jacob, Elsadig Mahdi Ahmed, Mohd. Sapuan Salit[1] and M. Saleem

Aerospace Engineering Department, University Putra Malaysia.

[1]Mechanical Engineering Department, University Putra Malaysia.

ABSTRACT

A detail survey of the existing fretting fatigue test equipments used is given and a new fretting fatigue test apparatus has been designed and fabricated. The fretting fatigue test apparatus permits the examination of the contact zone during the test and allows the precise measurement of frictional force induced at the contact interface due to the fretting action. The fretting fatigue experiments have been carried out using 7075-T6-aluminium alloy specimen with the En24 steel pad with flat over flat contact condition. It has been observed that the life reduction factors increase with increase in normal stress for given maximum axial stress. For the specimens tested under fretting fatigue condition with normal stress in the range of 45 MPa to 90 MPa the average life reduction factors are 12.52, 6.71, and 2.28 for maximum axial stresses of 290 MPa, 300 MPa, and 325 MPa respectively. The micro cracks along the contact interface below the pads have been nucleated and these micro cracks later on link to other cracks to form a composite major crack which is considered as a leading cracks through the thickness, while other will be considered as non-propagating cracks. The crack initiation of the order of 20 micrometer is captured with the help of video microscope.

Keywords : *Fretting fatigue, Test apparatus, Calibration, Frictional force, S-N curve*

INTRODUCTION

Many aerospace structures have sub-assemblies of different parts with contacting surfaces under pressure. When such assemblies are subjected to external cyclic axial loads, relative displacement of very small amplitude takes place at the contacting surfaces. This relative displacement induces frictional force at the contact zone. The combination of contact pressure, frictional force and external cyclic axial load develops a localised stress field at the contact interface, which leads to early nucleation of micro cracks. Subsequently under the action of the localised stresses these micro cracks will grow leading to failure. The process of crack initiation and propagation at the contact interface due to the resulting localised stresses is termed as fretting fatigue. The schematic illustration of fretting fatigue in the contacting bodies with anticipated loading is shown in Figure 1. The fretting damage has been observed in a number of practical situations e.g. riveted joints Buch [1], Szolwinski et al [2]; bolted plates and wire ropes Forsyth [3]; biomedical implants Adibnazari and Hoeppner [4], Mutoh [5]; micro mechanical devices, and ball bearings Mugadu and Hills [6], Navaro et. al. [7].

In 1911 Eden [8] noted the formation of oxides inside the grips of the fatigue test specimen which led the way for the development of fretting fatigue studies. The first formal experiments about fretting fatigue were done by Tomlinson [9] and their work has led to an important conclusion that the fretting fatigue damage is mainly responsible due to relative motion between the two contacting surfaces. The debate is still on even after decades of experimental research work in fretting fatigue to standardise the fretting fatigue test apparatus as per the summary article by Waterhouse [10].

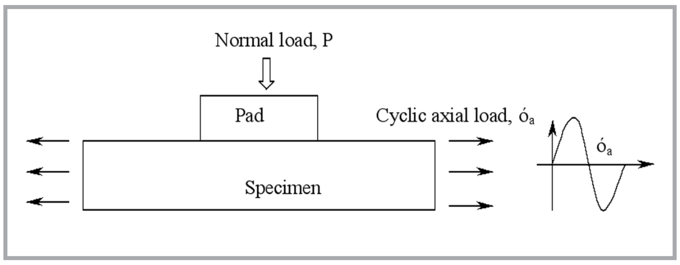

Figure 1: Schematic illustration of fretting fatigue loading

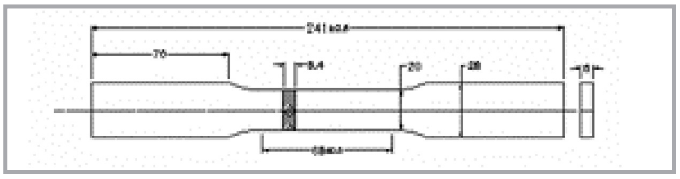

(a) Specimen

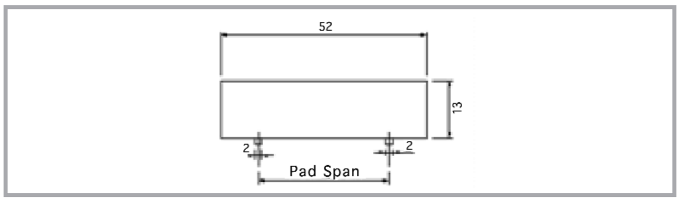

(b) Pad

Figure 2: Geometrical details of the specimen and Pad

The objective of the present investigation is to present a detailed survey of the fretting fatigue test rigs used and to present a new design of fretting fatigue test rig system with a facility to view the crack nucleation zone under fretting fatigue loading condition. Also it is envisaged to present the detailed experimental fretting fatigue test procedure. In addition it is planned to carry out fretting fatigue tests to study the effect of normal stress on the fretting fatigue life characteristics.

MATERIALS AND SPECIMEN

The material used for the fretting fatigue test specimens is 7075-T6 aluminium alloy and for the pad is En24 steel. The mechanical properties of the specimen and pad materials are given in Table 1. The geometrical details of the specimen and pad are given in Figure 2.

Test procedure

The fretting fatigue tests are conducted on a 100kN servo hydraulic material test system. The specimen is mounted rigidly in the recess of the test rig and the fretting pads are carefully aligned at the centre of the specimen gage section. Once the fretting pads along with the load train are mounted over the specimen the whole specimen assembly is transferred to the grip system of the MTS machine and thereby the

Table 1: Mechanical Properties

Mechanical Properties	7075-T6 aluminium alloy	En24 steel
Young's Modulus, MPa	69000	200000
Yield strength, σ_y (0.2%), MPa	522	245
Ultimate Strength, σ_u, MPa	575	510
Poisson's ratio, ν	0.33	0.33

specimen is gripped. The two normal load cells and two frictional force load cells are connected to data acquisition system for recording normal and frictional load. The normal load is applied to the specimen through the pads by turning the loading screw provided in the test rig. Now the test rig is ready for carrying out the experiment. After applying the normal load through the pads a cyclic axial load corresponding to axial stress is applied to the specimen through the MTS system. The test is conducted with load mode condition of the MTS machine. The tests are carried out with R = 0.1 and with test frequency of 10 Hz. The variation of the applied normal load through the pads is monitored regularly to check if there is any variation in its value. The frictional force values are recorded frequently at the beginning of the experiment (first few hundred cycles) till its stabilisation. Thereafter the frictional force data is recorded over an interval of 10,000 cycles.

DIFFERENT TYPES OF TEST RIG

In most of the fretting fatigue test apparatus design there is facility of cyclic axial load application to the specimen along with a constant lateral normal load and the tangential load parallel to the axis of the specimen. A few different types of test rigs with their loading mechanisms are described in the following paragraphs.

Mechanical devices such as eccentric cam mechanisms (Figure 3) are used by some researchers Kayaba and Iwabuchi [11], Waterhouse et al. [12], and Niu et.al. [13] which apply cyclic axial load to the specimen. The transverse normal load is applied to the specimen by placing weights on a counter body holder which induces frictional force at the contact interface. The cyclic axial load induces relative displacement at the pad-specimen interface and it counteracts the frictional force at the contact interface. A piezoelectric transducer is attached to the counter body holder for measuring the frictional force developed at the contact interface. The frictional force and the cyclic axial load data's are fed to the digital oscilloscope for recording and monitoring the test parameters during the experiment.

Koenen et al. [14] used a different set up as shown Figure 4 in which a frequency generator is used to generate the actuator excitation signal. A closed loop feedback control system is used to maintain either constant amplitude of displacement, force, acceleration or speed. The same type of system maintains the position of the sample constant with respect to some datum level. This system is independent of frequency and loading conditions. The set point controls adjust the excitation voltage and position of the contact. The machine can test specimens with repeatable experimental conditions. Adjusting these control conditions and the variable range of frequencies available, tests can be performed which can simulate many fretting applications Now the test rig is ready for carrying out the experiment in engineering.

Dubourg et al. [15] designed a fretting fatigue test rig for polymer materials as shown in Figure 5. Here the specimen is clamped between grips and the cyclic axial load is applied by means of a connecting rod-crank mechanism. The cylindrical pad applies normal load on to the specimen. The photoelastic system is used to measure the crack length, which is composed of a light source and two polariscopes, located perpendicularly to the lateral faces of the transparent epoxy material, which is mounted on the surface of the specimen. The associated isochromatic fringe patterns are filmed using a charge coupled device (CCD) camera. A model was developed to analyse the digitalised images, which determine the exact geometry and length of the cracks. Hence the evolution of cracks (length, inclination) was recorded and both qualitative and quantitative data were obtained.

A single experimental setup capable of performing fretting fatigue tests in laboratory air environment or in a scanning electron microscope (SEM)

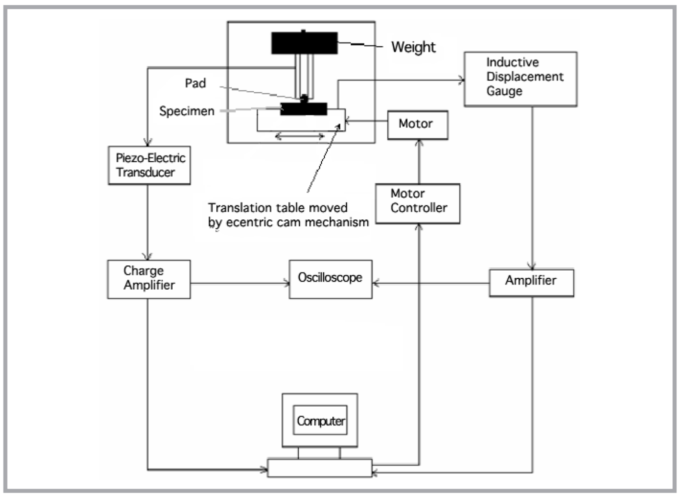

Figure 3: Schematic illustration of eccentric cam mechanism fretting apparatus

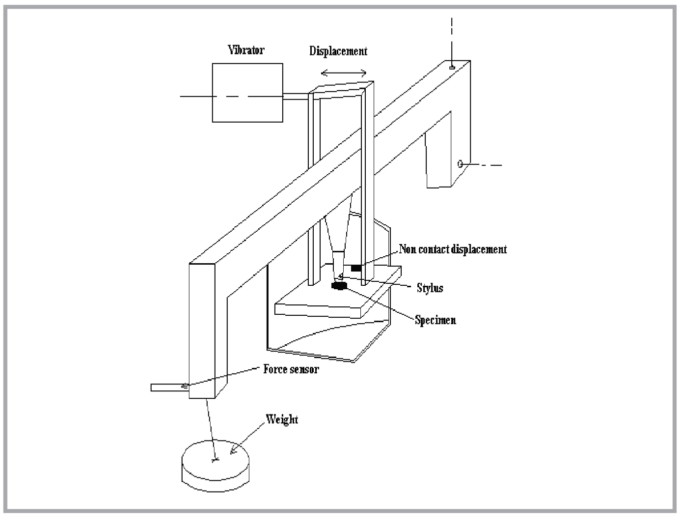

Figure 4: Vibro-Cryo-Tribometer cum fretting fatigue appaatus

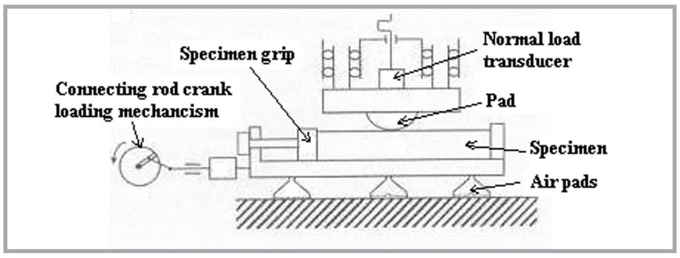

Figure 5: Fretting fatigue test apparatus for polymer materials

vacuum environment has been developed by Elliot and Hoeppner [16] as shown in Figure 6. The fretting fatigue test rig consists of external fatigue loading, internal fatigue loading, internal fretting loading and vacuum lid subsystems. The external fatigue loading subsystem, which is outside the SEM, allows the fatigue load to be transmitted to the specimen inside SEM.

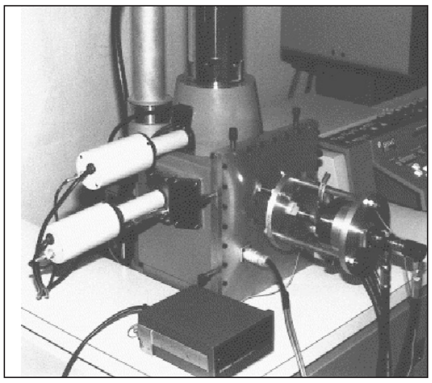

Figure 6: Fretting fatigue test apparatus in SEM environment

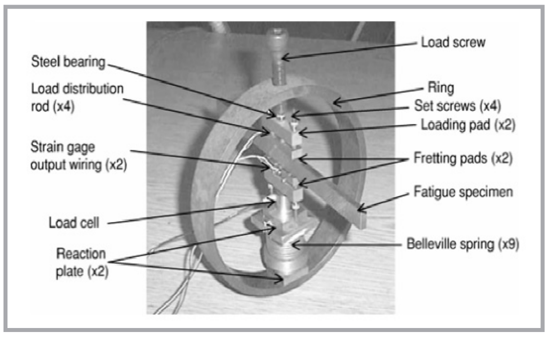

Figure 7: Ring type fretting fatigue test apparatus

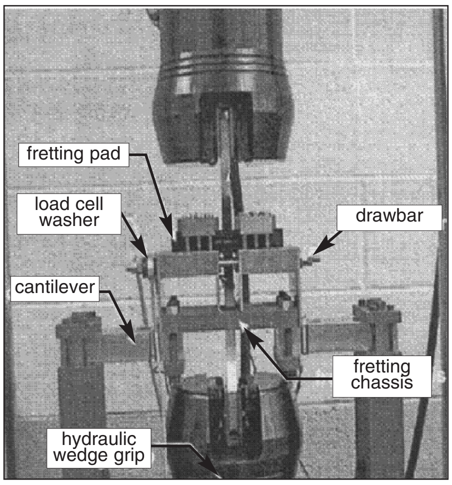

Figure 8: Fretting fatigue text apparatus with single actuator servo hydraulic system

It also has an arrangement to move the specimen further into the SEM chamber for viewing the contact zone. The internal fatigue loading subsystem applies fatigue loading to the specimen. The internal fretting loading subsystem applies normal load to the specimen through fretting pads. The vacuum lid subsystem has a provision to move the specimen left, right and up directions within the SEM chamber. All interfaces between outside and inside of the vacuum chamber are in the vacuum lid subsystem.

A ring type fretting fatigue test apparatus (Figure 7) has been developed by Wallace and Neu [17]. The servo hydraulic material testing system applies the cyclic axial load to the specimen, which is mounted on the system with fretting attachment. The normal load to the specimen is transmitted through a calibrated proving ring. The loading screw applies normal load to the centre of the loading pad through a solid carbide ball and thereby the load is transferred to the fretting pad holder through two cylinders located over the centre of the fretting pad holder and finally to the specimen through the two fretting pads. Belleville spring located at the opposite end of the loading screw helps to maintain a constant normal load between pads and the specimen. An external data acquisition system was used to record the cyclic axial load applied to the specimen and the induced fictional force at the contact interface due to the normal load applied to the specimen.

Hydraulic single actuator mechanisms are utilised (Nowell and Hills [18], Szolwinski and Farris [19], Wittkowsky et al. [20]) to apply the cyclic axial load to the specimen. At the same time the normal load to the specimen is applied by means of an additional mechanical fixture as shown in Figure 8. A chassis holding the fretting pads is connected to two beam structures and then mounted on a set of uprights bolted to the load frame platform. A set of drawbars passed through the chassis is used to apply the normal load to the pads. A computer based data acquisition system is used to acquire and store the fretting fatigue test parameters. Advantages of this type of configuration are easy control of specimen cyclic axial load and flexible use of different types of pad geometries.

Since the fretting damage at the contact zone leads to early failure of the material a closer examination of the contact zone and measuring the loads acting at the contact interface helps to understand the fretting process. It is clear from the literature survey that a meagre research work has been carried out to stress the behavioural changes of the material around the contact interface. In view of this a new fretting test rig has been designed and fabricated to characterise the material behaviour under fretting fatigue in particular around the contact region.

FRETTING FATIGUE TEST RIG

The fretting fatigue test rig has been designed and it is to be used with 810 MTS servo- electro-hydraulic single actuator material test system of 100 KN capacity. Figure 9 shows the assembly of fretting fatigue test rig. Loading jig (1) is the rigid base in which load cells, pad holders and specimen are mounted. An under cut of 2 mm deep is machined at the base of the loading jig to facilitate proper seating of the load cell-A (3). The position of the load cell-A can be adjusted for different pad heights and can be screwed over the base of the loading jig (1). In the loading jig (1) a recess equal to the width of the specimen is machined to facilitate mounting of specimen (10). The two loading pad holders are fixed to two-load cells-A (3) and they are located symmetrically over the specimen in the longitudinal direction i.e. in the direction of the stroke of the machine. The loading jig (1) and the specimen (10) are fixed rigidly by a loading plate (2) through the bolts. Below the specimen (10) a spacer is provided to align the centre of the specimen and machine grips to cater different thickness of the specimens. Pads (9) are held by the pad holders (6). One end of the pad holder is screwed to load cell-A (3) and it acts a load-transferring link to the load cell-A (3), which will help to measure the frictional force around the contact zone. Normal load to the pads is applied through the load cell-B (7) by turning the loading bolt (4). The auxiliary loading block (5) distributes the load equally at two locations over the loading pin (8), which is directly above the pads (9). Both load cells A (3) and B (7) are calibrated individually to measure the normal and frictional force at the contact interface.

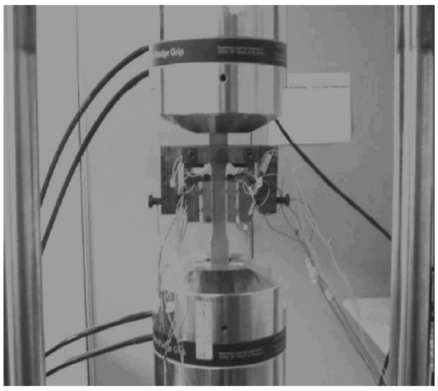

Figure 9: (a) Fretting fatigue rig shown mounted on MTS material test system

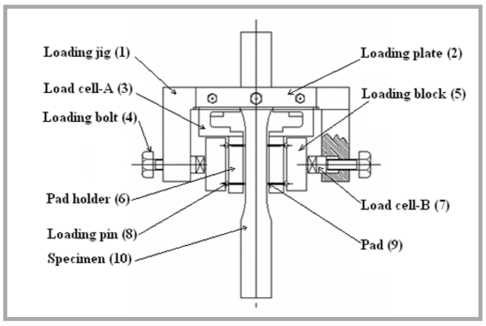

Figure 9: (b) Schematic Illustration

A Video Microscope (VM) is utilised for observing the crack nucleation as a result of changes in the material behaviour around the contact region

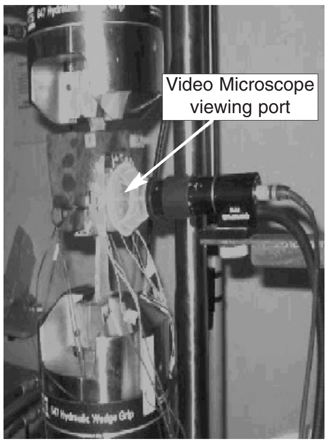

Figure 10: Video microscope set up

and is shown in Figure 10. The Video Microscope has the facility to view the region with a magnification in the range of 70X to 200X. The Video Microscope viewing port can be positioned at any time at the contact zones to view and record the crack initiation region and take photographs of the cracked sample at the predefined number of cycles. The induced frictional force/tangential load at the contact zone is measured by the frictional force load cell. The design incorporates the advantages of other fretting fatigue assemblies reported in this paper. The notable advantages are interchangeable fretting pads, the facility of using pads with different heights, and fretting fatigue test with two pads testing having a variable pad span.

CALIBRATION OF LOAD CELLS

Load cell-A

Load cell-A is calibrated to measure the frictional force at the contact interface. For calibration of load cell-A a separate fixture has been designed and fabricated is shown in Figure 11. The load is applied to the loading pin. The applied load is transferred to the load cell-A through the loading block. Four strain gauges are pasted on each load cell-A to measure the strains due to the applied load. The strain gauges are connected to form a Wheatstone bridge circuit and the same is connected to dynamic strain indicator (DPM-713B) through bridge box (DBB-120). Load is applied gradually to the load cell-A and the strain indictor reading is noted down at every 500 N load intervals. Applied load versus the measured bridge output voltage values is plotted and is shown in Figure 12. The calibration constant for right load cell-A is 5501.3 N per voltage and for left load cell-A is 5377.8 N per voltage. During the experiment the readings of the load cells-A are taken and the required frictional force at the contact is obtained by the respective load cells-A.

Figure 11: (a) Load cell-A Calibration Fixture

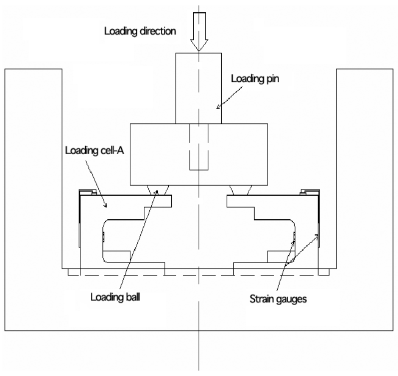

Figure 11: (b) Schematic illustration

Load cell-B

Load cell-B is calibrated to measure the normal load applied to the pads. The calibration fixture indicating the mode of load application is shown in Figure 13. The load is transferred to the load cell-B through the loading pin. A cylindrical spacer connects the two-load cells-B. The Wheatstone bridge circuit over the load cell-B is made using the strain gauges as described in the preceding paragraph. Following the procedure of load cell-A calibration the Load cell-B is also calibrated (Figure 14). The calibration constant for Top load cell-B is 8227.2 N per volt and for bottom load cell-B is 8879.4 N per volt. The normal load on the respective side of the specimen is monitored through the corresponding load cells-B.

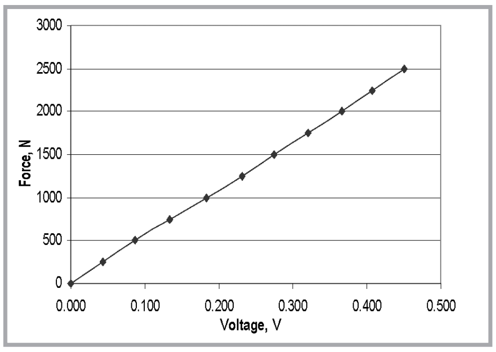

(a) Right Load Cell-A

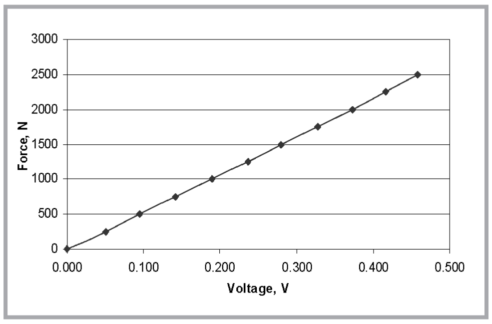

(b) Left Load Cell-A

Figure 12: Load Cell-A calibration graph

Figure 13: (a) Load Cell-B calibration fixture

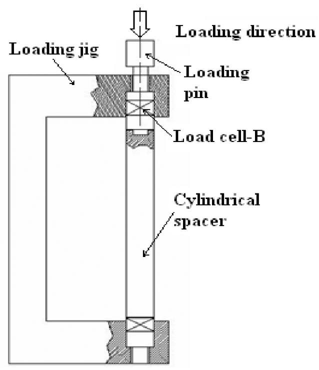

Figure 13: (b) Schematic illustration

RESULTS AND DISCUSSIONS

The fatigue tests and fretting

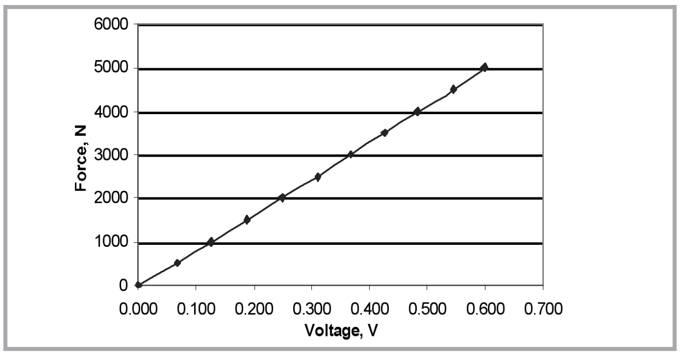

(a) Top Load Cell-B

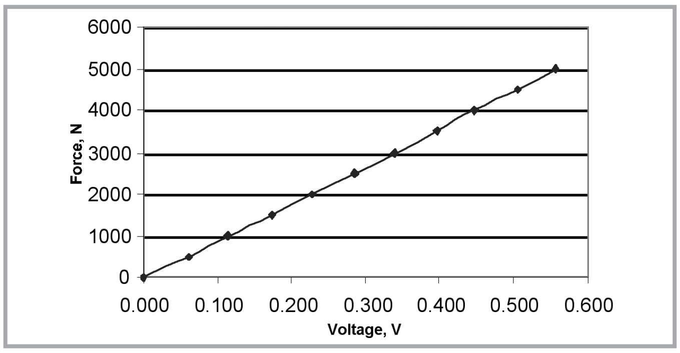

(b) Bottom Load Cell-B

Figure 14: Load Cell-B Calibration Graph

fatigue tests were conducted on 7075-T6 aluminium alloys at three maximum axial stresses of 290 MPa, 300 MPa, and 325 MPa with a stress ratio R of 0.1. For fretting fatigue tests, three normal stresses 45 MPa, 60 MPa, and 90 MPa were used along with the maximum axial stress. The results of the fretting fatigue tests and of plain fatigue tests are given in Table 2. The relative representative S-N curves for the plain fatigue tests and fretting fatigue tests are shown in Figure 15. At 290 MPa axial stress the fatigue life of the specimens is in the range of $9.3x10^5$ to $3.2 x10^6$ cycles, whereas the fatigue lives for two specimens tested at each stress level with fretting stresses of 45 MPa, 60 MPa, and 90 MPa are 2.44658 x 10^5, 2.35892 x 10^5; 1.47758x 10^5, 1.42318 x 10^5; 1.06317x 10^5, 0.94758 x 10^5 cycles respectively. The median fatigue life for plain fatigue test

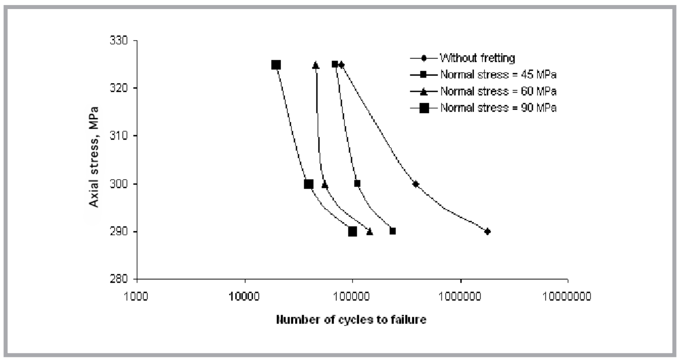

Figure 15: The Representative S-N curve for 7075-T6-aluminium alloy (R = 0.1, f = 10Hz)

case for an axial stress of 290 MPa is $1.785548x10^6$ cycles. The fatigue life reduction factors are calculated based on the median life of plain fatigue tests at each stress level. The fatigue life reduces by a factor of 7.43, 12.32, and 17.82 respectively for maximum axial stress of 290 MPa due to normal stress of 45 MPa, 60 MPa, and 90 MPa. The life for plain fatigue test specimens tested at 300 MPa maximum axial stress is in the range of 3.48508 x 10^5 to 3.99589 x 10^5 cycles. The median life for plain fatigue life tests at maximum axial stress of 300 MPa is 3.85581 x 10^5 cycles. The fatigue lives for two specimens tested at each stress level due to fretting at normal pressures of 45 MPa, 60 MPa, and 90 MPa the life

Table 2: Fretting fatigue and plain fatigue results for 7075-T6 aluminium alloys for various maximum stress levels and various normal stresses (R = 0.1, freq. = 10Hz)

S.No.	Specimen number	Max. axial stress, MPa	Normal Stress, MPa	Cycles to failure, N_f	Life reduction factor
	290A	290	Plain fatigue	931665	-
	290B	290	Plain fatigue	1186312	-
	290C	290	Plain fatigue	2384785	-
	290D	290	Plain fatigue	3204068	-
	29045A	290	45	244658	7.298
	29045B	290	45	235892	7.569
	29060A	290	60	147758	12.084
	29060B	290	60	142318	12.546
	29090A	290	90	106317	16.794
	29090B	290	90	94758	18.843
	300A	300	Plain fatigue	399589	-
	300B	300	Plain fatigue	385581	-
	300C	300	Plain fatigue	348508	-
	30045A	300	45	111549	3.456
	30045B	300	45	110896	3.477
	30060A	300	60	56086	6.875
	30060B	300	60	55947	6.892
	30090A	300	90	39420	9.781
	30090B	300	90	39358	9.797
	325A	325	Plain fatigue	91270	-
	325B	325	Plain fatigue	77810	-
	325C	325	Plain fatigue	69005	-
	32545A	325	45	69926	1.113
	32545B	325	45	68742	1.132
	32560A	325	60	45385	1.714
	32560B	325	60	44978	1.730
	32590A	325	90	19972	3.896
	32590B	325	90	19050	4.084

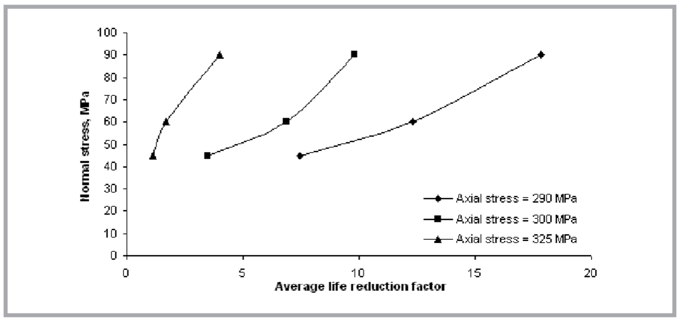

Figure 16: Normal stress vs. Life reduction factor under fretting fatigue for 7075-T6 (R = 0.1, f = 10Hz)

reduces to 1.11549 x 10^5, 1.10896 x 10^5; 0.56086 x 10^5, 0.55947 x 10^5; 0.39420 x 10^5, 0.39358 x 10^5 cycles respectively.

The life reduces by factors of 3.47, 6.88, and 9.79 respectively for normal stress of 45 MPa, 60 MPa, and 90 MPa along with a 300 MPa maximum axial stresses.

Similarly it is observed that the fatigue life at axial stress of 325 MPa is the range of 0.69005 x 10^5 to 0.9127 x 10^5 cycles. The median life for plain fatigue life tests at maximum axial stress of 325 MPa is 0.77810 x 10^5 cycles. The fatigue lives for two specimens tested at each stress level due to fretting at normal pressures of 45 MPa, 60 MPa, and 90 MPa for maximum axial stress of 325 MPa are 0.69926 x 10^5, 0.68742 x 10^5; 0.45385 x 10^5, 0.44978 x 10^5; 0.19972 x 10^5, 0.19050 x 10^5 cycles respectively.

The fatigue life reduces by a factor of 1.122, 1.72, and 3.99 respectively for normal stresses of 45 MPa, 60 MPa, and 90 MPa at maximum axial stress of 325 MPa. The life reduction factors for fretting fatigue test specimens tested at three maximum axial stresses with 45 MPa, 60 MPa, and 90MPa normal stresses are shown in Figure 16. It is observed that the life reduction factors increase with increase in normal stress. The life reduction factors themselves reduce as the maximum axial stress is increased. The average life reduction factors are 12.52, 6.71, and 2.28 for maximum axial stresses of 290 MPa, 300 MPa, and 325 MPa respectively for specimens tested under fretting fatigue condition. In general at higher axial stress the spread between the fretting fatigue life and fatigue life is small while at lower axial stress level the difference is very large. The same behaviour is observed by Goss and Hoeppner [22] for the 7075-T6 aluminium alloy specimen for different loading condition.

SCANNING ELECTRON MICROSCOPE STUDY

The scanning electron micrographs for one of the specimen tested under fretting fatigue with maximum axial stress of 300 MPa and a normal stress of 60 MPa is shown in Figure 17. The typical fretting contact scars generated during the fretting fatigue test shows the damage under partial stick and slip condition where the stick regions is surrounded by slip regions. It is observed from the SEM micrograph that there exists rippling at A1, delamination at A2 and ploughing at A3 (Figure 17). Also at a location B in the SEM micrograph (Figure 17) micro cracking is seen at the contact interface. A numbers of secondary cracks are also formed parallel to one another in the whole fretted region and the same behaviour is also reported in reference Alic et.al [23]. These secondary cracks are associated with the plastic deformation at the contact interface due to fretting action.

The cracks are nucleated along the contact interface below the pads and are shown in Figure 17 at location B. The enlarged view of the micro cracks with respect to point B (Figure 17) is shown in Figure 18. These micro cracks under fretting fatigue-loading condition propagate during the test individually and later on link to other cracks to form a composite major crack, which will be considered as a leading crack while other cracks, will be considered as non-propagating cracks. The leading crack will start appearing on the lateral surface of the specimen, which is not subjected to fretting, and this crack may run through the thickness of the specimen. As far as fretting and fatigue crack propagation is concerned the first appearance of the cracks on this lateral surface is termed as crack initiation. The crack initiation is captured with the help of video microscope. In Figure 19 a small crack of the order of 800 mm is captured. The fracture mechanics analysis of the

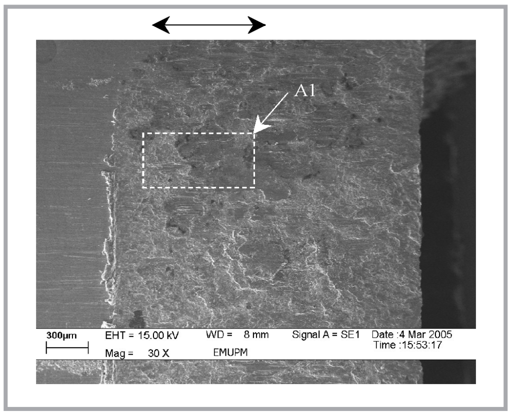

Figure 17: (a) Fretting fatigue scar at 30X magnification

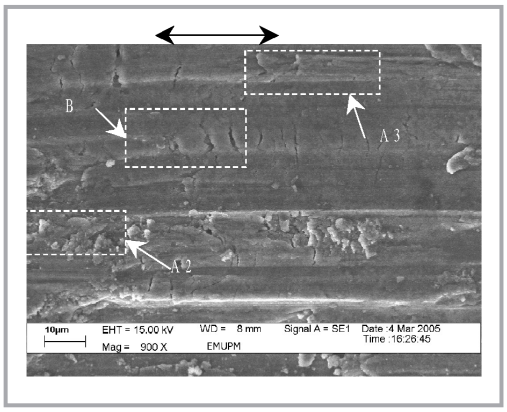

Figure 17: (b) Fretting fatigue crack observed at the specimen surface. The arrows indicate the loading direction.

Figure 17: Scanning electron microscope micrograph (cyclic axial stress = 300MPa, normal stress = 60 MPa, R = 0.1, frequency = 10Hz)

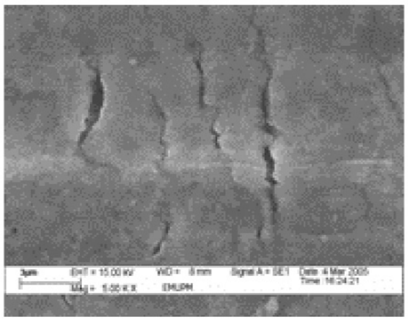

Figure 18: Multiple cracks under fretting fatigue at a location B (Figure 17)

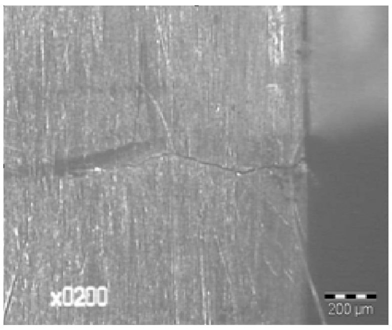

Figure 19: Video microscope image of a propagated crack captured during experiment. (Cyclic axial stress = 300MPa, Normal stress = 60 MPa, R = 0.1, f = 10Hz)

propagating cracks under fretting fatigue condition is being presented in another paper.

CONCLUSION

Following conclusions are presented from the present study,

i) A new fretting fatigue test apparatus has been designed and fabricated. The fretting fatigue test apparatus permits the examination of the contact zone during the test. It allows precise measurement of frictional force induced at the contact interface due to the fretting action.

ii) The life reduction factors increase with increase in normal stress for given maximum axial stress.

iii) The average life reduction factors are 12.52, 6.71, and 2.28 for maximum axial stresses of 290 MPa, 300 MPa, and 325 MPa respectively for specimens tested under fretting fatigue condition with normal stress in the range of 45 MPa to 90 MPa.

iv) A crack of the order of 20 micrometer can be measured using the video microscope for specimens subjected to fretting fatigue loading.

ACKNOWLEDGEMENTS

The authors gratefully acknowledge the financial support of the Ministry of Science and Technology & Environment, Malaysia (IRPA Project No-09-02-04-0446-EA001) for the provision of research grant for this work. ■

REFERENCES

[1] A., Buch, Fatigue and fretting of pin-lug joints with and without interference fit, Wear, 43, 9-16, 1977

[2] M.P., Szolwinski, G., Harish and P.A., Mc Veigh and T.N., Farris, The role of fretting fatigue crack nucleation in the onset of widespread fatigue damage: Analysis and experiments, FAA-NASA Symposium on the Continued Airworthiness of Aircraft Structure, Atlanta, 585-596, 1996

[3] P.J.E., Forsyth, Occurrence of fretting failure in practice, Fretting fatigue, ed. Waterhouse, R.B, Applied Science Publishers, London. 99-125, 1981

[4] S., Adibnazari and D.W., Hoeppner, A fretting fatigue normal pressure threshold concept, Wear, 160, 33-35, 1993

[5] Y., Mutoh, Mechanism of fretting fatigue, JSME International Journal Series A, 38, 405-415, 1995

[6] A., Mugadu, and D.A., Hills, A generalized stress intensity approach to characterizing the process zone in complete fretting contacts, International Journal of Solids and Structures, 39, 1327-1335, 2002

[7] C., Navarro, M., Garcia and J., Domiguez, A Procedure for estimating the total life in fretting fatigue, Fatigue Fracture Engineering Material Structure, 26, 459-468, 2003

[8] E.M., Eden, W.N., Rose and F.L., Cunningham, The endurance of metals, Proceedings of the Institution for Mechanical Engineers, 4, 839-974, 1911

[9] G.A., Tomilson, The rusting of steel surfaces in contact, Proceedings of the Royal Society, London, Series A, 115, 472-483, 1927

[10] R.B., Waterhouse, The problems of fretting fatigue testing, in: M.H. Attia, R.B. Waterhouse (Eds.), Standardization of fretting fatigue test methods and equipment, ASTM STP 1159, American Society for Testing and Materials, Philadelphia, PA, 13-19, 1992

[11] T., Kayaba and A., Iwabuchi, Effect of the hardness of hardened steels and the action of oxides on fretting wear, Wear, 66, 27-41, 1981

[12] R.B., Waterhouse, I.R., Mccoll, S.J., Harris and M., Tsujikawa, Fretting wear of a high-strength heavily work-hardened eutectoid steel, Wear, 175, 51-57, 1994

[13] X.P., Niu, L., Froyen, C., Delacy and Peytour, Fretting wear of mechanically alloyed Al-Fe and Al-Fe-Mn alloys, Wear, 193, 78-90, 1996

[14] A., Koenen, P. H., Virmoux, R., Gras, J., Blouet, J.M., Dewulf and J.M., Demonicault, A machine for fretting fatigue and fretting wear testing in cryotechnical and normal environment, Wear, 197, 192-196, 1996

[15] M.C., Dubourg, A., Chateauminois and B., Villechaise, In situ analysis and modelling of crack initiation and propagation within model fretting contacts using polymer materials, Tribology International, 36, 109-119 2003

[16] C.B., Elliott III and D.W., Hoeppner. The importance of wear and corrosion on the fretting fatigue behaviour of two aluminium alloys, Wear, 236, 128-133, 1999

[17] J.M., Wallace and R., Neu, Fretting fatigue crack nucleation in Ti-6Al-4V, Fatigue Fracture Engineering Materials Structure, 26, 199-214, 2003

[18] D., Nowell and D.A., Hills, Crack initiation criterion in fretting fatigue, Wear, 136, 329-343, 1990

[19] M.P., Szolwinski and T.N., Farris, Observation, analysis and prediction of fretting fatigue in 2024-T351 aluminium alloy, Wear, 221, 24-36, 1998

[20] B.U., Wittkowsky, P.R., Birch, J., Dominguez and S., Suresh. An apparatus for quantitative fretting fatigue testing, Fatigue Fracture Engineering Material Structure, 22, 307-320, 1999

[21] Olof Vingsbo and Staffan Soderberg, On fretting maps, Wear, 126, 131-147, 1988

[22] G.L., Goss and D.W., Hoeppner. Normal load effects in fretting fatigue of titanium and aluminium alloys, Wear, 27, 153-159, 1974

[23] J.A., Alic; A.L., Hawley and Judy M.Urey. Formation of fretting fatigue cracks in 7075-T7351 aluminium alloy, Wear, 56, 351-361, 1979.